



JOINT INSTITUTE FOR NUCLEAR RESEARCH
Veksler and Baldin laboratory of High Energy Physics

FINAL REPORT ON THE INTEREST PROGRAMME

*Soft Photon study in hadron and nuclear
interactions*

Supervisor:

Prof Elena Kokoulina

Student:

Milena Micic, Serbia
University of Belgrade

Participation period:

September 27 – November 05, Wave 5

Dubna, 2020

Contents

| | |
|---------------------------------|-----------|
| Introduction | 3 |
| Project goals | 3 |
| Particle detection | 3 |
| 3.1. Bremsstrahlung | 3 |
| 3.2. Pair production | 4 |
| 3.3. Electron-photon cascades | 5 |
| Calorimeters | 6 |
| 4.1. Homogeneous calorimeters | 6 |
| 4.2. Heterogeneous calorimeters | 7 |
| Simulation | 8 |
| 5.1. Homogeneous calorimeter | 8 |
| 5.2. Spaghetti type calorimeter | 9 |
| Conclusion | 11 |
| References | 11 |
| Acknowledgments | 11 |

1. Introduction

Soft photons are the direct products of high-energy interactions, with energies smaller than 50 MeV. Experiments have shown an excess yield of soft photons in hadron and nuclear interactions. Even though those experiments were done more than thirty years ago, there is still no comprehensive explanation for this phenomenon.

One way of detecting soft photons is by using Electromagnetic calorimeters. When an incident particle, in this case a soft photon, enters the calorimeter, an electron-photon cascade is created. This implies total absorption of particle energy in the material as well as a measurement of the deposited energy by placing a light detector, usually a Silicon photomultiplier (SiPM), at the end. There are two types of such calorimeters: homogeneous, which are made of one type of material that behaves as an absorber and detector at the same time, and heterogeneous or sampling calorimeters, consisting of two different materials.

In this paper, two types of sampling calorimeters are compared - spaghetti and shashlik. Different types and thicknesses of absorber materials are discussed as well as eliminating the absorber material altogether (homogeneous calorimeter).

The simulation is conducted using the Monte-Carlo method based on Example 4 in GEANT4. All figures and curve fittings were done using CERN Root.

2. Project goals

The goal of this project is to firstly, study the theoretical basis of particle detection by calorimetry. Then, simulate different types of calorimeters for soft photon detection using the Monte-Carlo method in GEANT4. For this step, the simulation is built on the basis of Example 4 in GEANT4. Once simulated successfully it is necessary to calculate energy resolution for every model. Comparison is done based on energy resolution and price of the detectors.

3. Particle detection

Particles can be detected only by interactions with matter. Depending on the type of interactions there are different types of particle detectors. One could even say that every interaction process can be a basis for a detector.

The main interactions of charged particles are ionization and excitation, and bremsstrahlung for relativistic particles. Neutral particles in interactions produce charged particles which could then be detected based on their characteristic interaction process. In the case of photons, these processes are Compton scattering, photoelectric effect, and pair production.

This report focuses on detecting soft photons using electromagnetic calorimeters, therefore the most important interactions to consider are bremsstrahlung for electrons and positrons, and pair production for photons, as they are the most dominant in electron-photon cascades at high energies (energies greater than 1 MeV).

3.1. Bremsstrahlung

Fast charged particles can lose energy in interactions with the Coulomb field of the nuclei of the traversed medium. If the charged particle is decelerated in the Coulomb field, a fraction of

their kinetic energy will be emitted in the form of a photon. The equation for energy loss by bremsstrahlung for high energies:

$$-\frac{dE}{dx} \approx 4\alpha N_a \frac{Z^2}{A} Z^2 \left(\frac{1}{4\pi\epsilon_0} \cdot \frac{e^2}{mc^2} \right)^2 \cdot E \ln \frac{183}{Z^{1/3}} \quad (3.1.1)$$

Where Z , A are the atomic number and weight of the medium, and z , m , E are the charge number, mass, and energy of the incident particle.

For an electron as the incident particle ($z = 1$ and $m = m_e$) we can define radiation length X_0 , as a property of a specific material:

$$-\frac{dE}{dx} = \frac{E}{X_0} \quad (3.1.2)$$

It can be calculated for a material composed of only one element:

$$X_0 = \frac{716.4 \cdot A}{Z(Z+1) \ln(287/\sqrt{Z})} \{g/cm^2\} \quad (3.1.3)$$

or for a mixture of elements:

$$X_0 = \frac{1}{\sum_{i=1}^N f_i / X_0^i} \quad (3.1.4)$$

Where f_i is the mass fraction of components with radiation length X_0^i :

$$f_i = \frac{A_i V_i}{\sum A_i V_i} \quad (3.1.5)$$

The energy at which energy loss for bremsstrahlung is equal to energy loss in ionization is called critical energy E_c .

$$E_c = \frac{550 \text{ MeV}}{Z_{eff}} \quad (3.1.6)$$

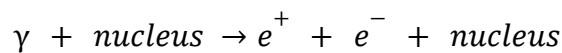
Where Z_{eff} is an effective atomic number for a material that is a mixture of elements:

$$Z_{eff} = \frac{\sum Z_i f_i}{\sum f_i} \quad (3.1.7)$$

The most common critical energy is around 10 MeV.

3.2. Pair production

Pair production is a characteristic photon interaction that occurs when a higher energy photon ($E_\gamma \gg 1 \text{ MeV}$) is found in the Coulomb field of the nuclei. It can be described as:



The cross-section for pair-production is given by:

$$\sigma_{pair} \approx \frac{7}{9} 4\alpha r_e^2 Z^2 \ln \frac{183}{Z^{1/3}} \approx \frac{7}{9} \frac{A}{N_A} \frac{1}{X_0} \quad (3.2.1)$$

3.3. Electron-photon cascades

From previous paragraphs, it can be determined that an electron or a positron loses on average 63.2% of its energy by bremsstrahlung over one radiation length. From the pair-production cross-section, it can be concluded that the mean free path for one pair production is $\frac{9}{7}$ of a radiation length.

The most important properties of electromagnetic cascades can be represented with a simpler model: both interactions, photon pair-production and electron or positron photon emission occur after one radiation length. It is assumed that the energy is symmetrically shared between particles at every step of the multiplication. Let t be the distance from the incident particle entering point normalized in radiation length $t = \frac{x}{X_0}$.

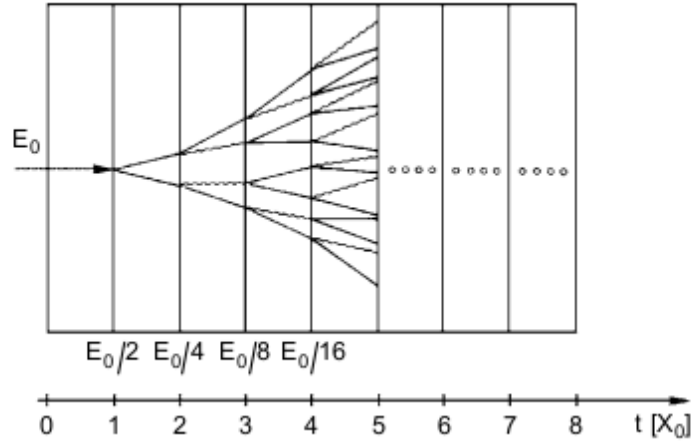


Fig. 3.3.1. A simple model for electromagnetic cascade

The energy of particles in generation t is:

$$E(t) = E_0 \cdot 2^{-t} \quad (3.3.1)$$

Multiplication of the shower particles continues as long as $E(t) > E_c$. For energies below critical energy absorption processes start to dominate. The position of a shower maximum can be calculated as:

$$t_{max} = \frac{\ln(E_0/E_c)}{\ln 2} \propto \ln(E_0/E_c) \quad (3.3.2)$$

The equation above represents longitudinal shower development of electromagnetic cascades.

To determine the lateral development of an electromagnetic shower only the multiple scattering effect should be considered. This width can be best characterized by the Moliere radius:

$$R_M = \frac{21 \text{ MeV}}{E_c} X_0 \{g/cm^2\} \quad (3.3.3)$$

4. Calorimeters

Calorimeters are particle detectors designed to fully absorb the energy of the incident particle. Using them it is able to measure the energy of the incident particle by absorption in the calorimeter, spatial location of energy deposition, and sometimes even the direction of the incoming particle.

Depending on the incident particle or the type of the calorimeter, electromagnetic or hadronic shower (cascade) is formed. As explained in the previous chapter, there are many charged particles in these showers that can ionize or excite the calorimeter medium. The ionization or excitation can cause a rise in visible photon emission (via scintillation) or in the release of ionization electrons. These phenomena can then be detected using photo-detectors or anodes/dynodes.

There are two general types of calorimeter geometries:

- homogeneous calorimeters
- heterogeneous calorimeters

Heterogeneous calorimeters can be electromagnetic or hadronic, while homogeneous calorimeters are almost exclusively for electromagnetic calorimetry. Since the focus of this report is on electromagnetic calorimeters they are the only ones that will be discussed moving forward.

One of the main parameters of electromagnetic calorimeters is energy resolution. The energy resolution is determined by both physical and technical factors. In this case, it is calculated based on experimental data:

$$\frac{\sigma(E)}{E} = \frac{\sigma_{Gauss} \cdot 100\%}{E_0} \tag{4.1}$$

Where σ_{Gauss} is the standard deviation for Normal distribution.

4.1. Homogeneous calorimeters

Homogeneous calorimeters are constructed using one material that performs as both an absorber and a detector. They are based on the measurement of scintillation light, ionization, and Cherenkov light. Materials usually used are scintillation crystals (PbWO₄, CsI(Tl), BGO, LYSO, and many others), liquid noble gases (Ar, Xe, Kr) for ionization as well as lead glass for Cherenkov light.

In this report, a homogeneous calorimeter with LYSO (Lu₂SiO₅) scintillation crystals is proposed. The main parameters for this material are given in the table:

| ELEMENT | ATOMIC NUMBER | ATOMIC WEIGHT | DENSITY [$\frac{g}{cm^3}$] | MASS FRACTION | RADIATION LENGTH [$\frac{g}{cm^2}$] | RADIATION LENGTH [cm] | VALENCE |
|---------|---------------|---------------|---------------------------------|---------------|--|-----------------------|---------|
| Lu | 71 | 174.967 | 9.841 | 0.764 | 6.95 | 0.71 | 2 |
| Si | 14 | 28.09 | 2.329 | 0.0613 | 22 | 9.4 | 1 |
| O | 8 | 16 | 1.43 | 0.175 | 34.46 | 24.097 | 5 |

Table 4.1.1. Parameters of elements found in LYSO crystal

Where f_i and X_0 are calculated using formulas 3.1.5 and 3.1.3. It is possible to calculate the radiational length of the LYSO crystal using this table and equation 3.1.4. That value is around 0,92 cm, which is significantly different from 1,2cm given in Table 5.2. in Particle Detectors in Groupen C. ([1]). This error is most likely due to approximations in equation 3.1.3.

Calorimeter dimensions could be calculated using equations 3.3.2 and 3.3.3. In the case of LYSO scintillation crystal as the calorimeter medium, the position of longitudinal shower maximum for electrons is $t_{max} = 1,038X_0$ and Molliere radius is $R_M = 2,157X_0$. Since these numbers are based on equations that assume certain approximations, a more efficient way of choosing calorimeter dimensions is through computer simulations, using the Monte-Carlo method.

4.2. Heterogeneous calorimeters

Heterogeneous calorimeters consist of two materials, one passive absorber, and one active detector. It is a compromise between having a bigger energy resolution at a smaller price than in the homogeneous calorimeters.

In this report, two types of heterogeneous calorimeters are proposed: spaghetti (figure 4.2.1, top) and shashlik (figure 4.2.1, bottom).

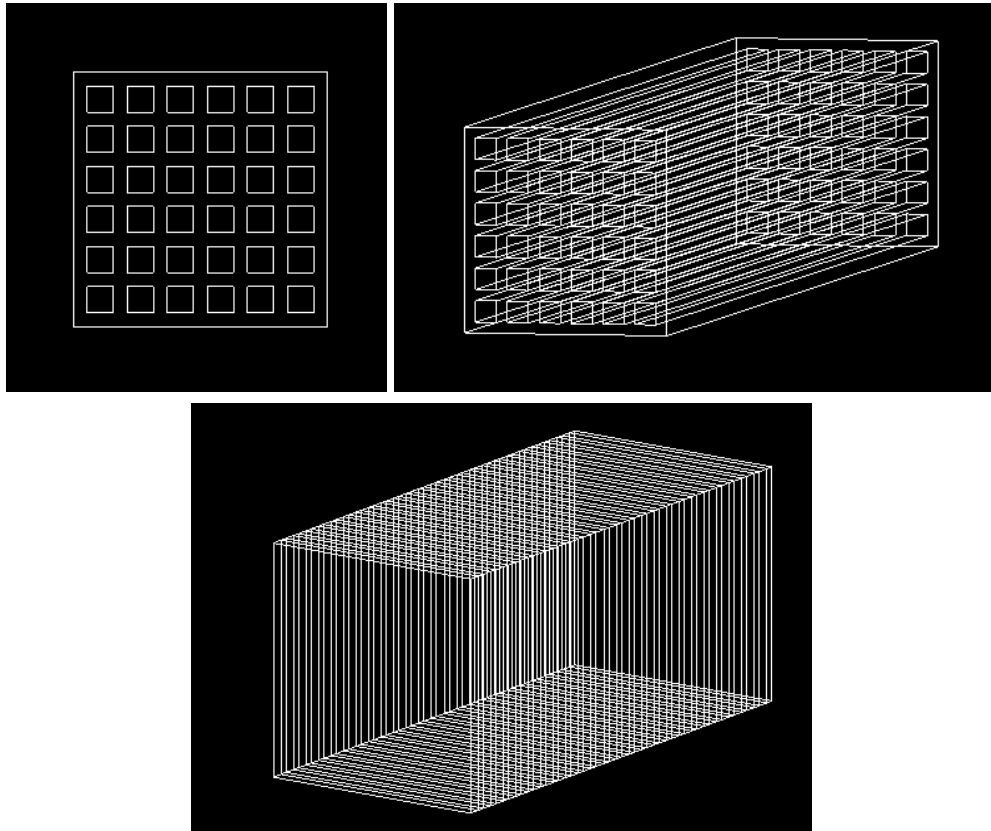


Fig. 4.2.1. Spaghetti type calorimeter (top), Shashlik type calorimeter (bottom)

The active detector material proposed is LYSO, described in the previous paragraphs. The passive absorber material proposed is a composite of Copper and Tungsten. Table 4.2.1 shows some of the characteristics of these two elements as well as the composite for three different mass ratios.

| ELEMENT/ COMPOSITE | DENSITY [$\frac{g}{cm^3}$] | RADIATION LENGTH [cm] |
|-----------------------|---------------------------------|-----------------------------|
| Cu | 8 | 1,43 |
| W | 15 | 0,35 |
| 5% Cu 95% W | 14,5 | 0,36 |
| 50% Cu 50% W | 11,5 | 0,56 |
| 95% Cu 5% W | 8,19 | 1,23 |

Table 4.2.1. Parameters of Cu, W and different composites of the two

In order to absorb as much of the particle energy as possible and therefore shorten the calorimeter thickness, the absorber material would ideally have to be very dense and with a small radiation length. However, using only Tungsten is very expensive. For the purpose of this simulation, a 50% Cu + 50% W composite is proposed, as a balance between the cost and density/radiation length.

The proposed spaghetti calorimeter consists of a passive absorber and scintillator rods laid out throughout the volume of the calorimeter, in the direction of the particle shower. In order to collect the emitted light, the scintillator rods are connected to a photomultiplier at the end. Proposed calorimeter has 27x27 rods equally spaced out, which makes the scintillator crystal about 24% of the calorimeter.

Proposed shashlik calorimeters consist of alternating layers of the passive absorber and active detector material. To collect the light emitted in the scintillator layers, wave-length shifter fibers are used throughout the calorimeter. In the first case, the ratio of the scintillator to absorber thickness is 1:3, which makes the scintillator about 25% of the total calorimeter volume. Then, the ratio 1:4 and 1:2 are proposed, which make the scintillator material 20% and 33% of the total calorimeter value respectively.

All of the calorimeters are simulated with the same total dimensions.

5. Simulation

All of the simulations were based on Example 4 in GEANT4, and all analysis, plotting and curve fitting were done using CERN Root.

In this report five types of electromagnetic calorimeters are simulated:

- homogeneous calorimeter, consisting of LYSO crystal only,
- spaghetti type calorimeter, consisting of about 24% of LYSO crystal and Cu+W composite
- shashlik type calorimeter, consisting of about 25% of LYSO crystal and Cu+W composite
- shashlik type calorimeter, consisting of about 20% of LYSO crystal and Cu+W composite
- shashlik type calorimeter, consisting of about 33% of LYSO crystal and Cu+W composite

5.1. Homogeneous calorimeter

The homogeneous calorimeter simulated consists of LYSO crystal only, which was described in Table 4.1.1. The total dimensions of the calorimeter are $55mm \times 55mm \times 120mm$. The energy deposition is given in Figure 5.1.1.

For larger energies, the figure shows only the beginning part of the fitted Gaussian distribution. The reason for this is the thickness of the calorimeter, which makes it unusable for larger energies. A way to resolve this problem is to enlarge the calorimeter thickness. As mentioned before, this solution is very cost-inefficient and that is why heterogeneous calorimeters are introduced.

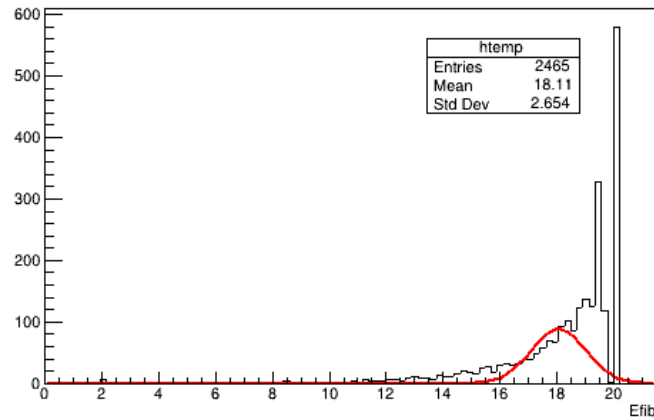


Fig. 5.1.1 Energy deposition of a homogeneous calorimeter for the energy of 20 MeV

As explained in equation 4.1, the energy resolution of the calorimeter for incident particle energy of 20 MeV can be estimated as:

$$\frac{\sigma(E)}{E} = 4.86\%$$

5.2. Spaghetti type calorimeter

The simulated spaghetti type calorimeter, described in chapter 4.2, consists of LYSO crystal as a scintillator and Cu+W compound as an absorber. Parameters for both of these materials are given in tables 4.1.1 and 4.2.1. The total dimensions of the calorimeter are $55\text{mm} \times 55\text{mm} \times 120\text{mm}$. Calorimeter consists of a 27×27 grid of scintillator rods. The dimensions of each rod are $1\text{mm} \times 1\text{mm} \times 120\text{mm}$, which makes the distance between every two rods 1mm . Energy

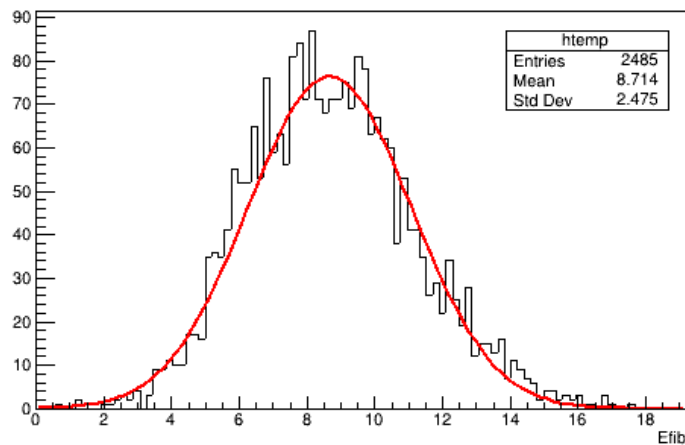


Fig. 5.2.1 Energy deposition of a spaghetti type calorimeter for the energy of 30 MeV

The energy resolution of the calorimeter for incident particle energy of 30 MeV can be estimated as:

$$\frac{\sigma(E)}{E} = 8.02\%$$

5.3. Shashlik type calorimeter

As is the case with spaghetti type calorimeters, all of the shashlik calorimeters, described in 4.2, consist of LYSO scintillator crystal layers alternating with Cu+W compound layers, acting as an absorber. In all three cases, thicknesses of the scintillator layers are 1mm , and thicknesses of absorber layers are 3mm , 4mm , and 2mm respectively. Total calorimeter dimensions are $55\text{mm} \times 55\text{mm} \times 120\text{mm}$. Figures and energy resolutions for all three types (3mm , 4mm , and 2mm) are given below.

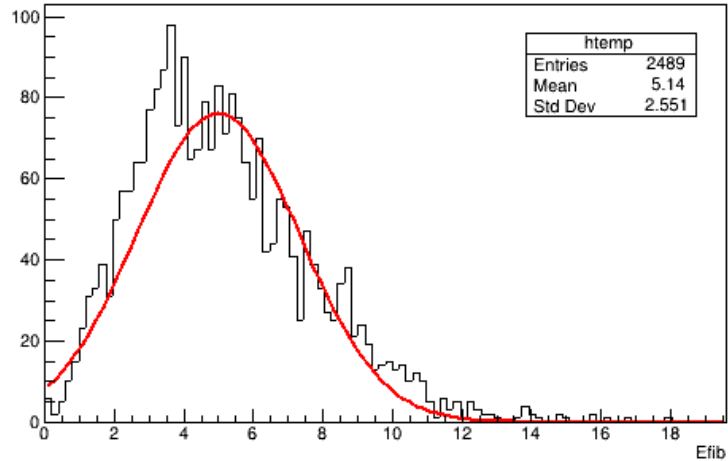


Fig. 5.3.1 Energy deposition of a shashlik type calorimeter with 3mm absorber thickness for the energy of 30MeV

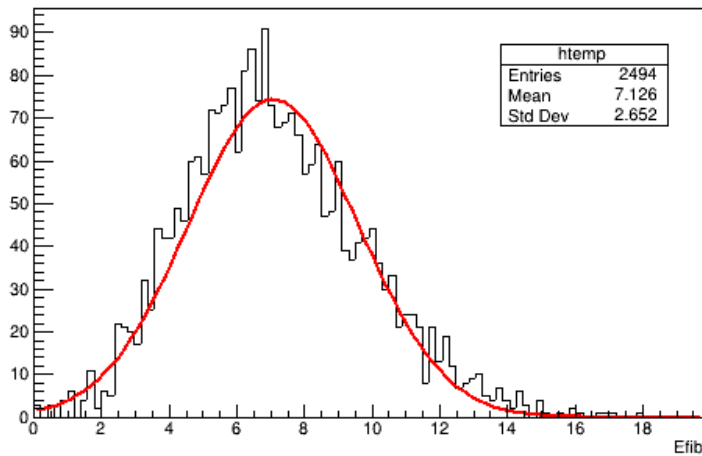


Fig. 5.3.2 Energy deposition of a shashlik type calorimeter with 2mm absorber thickness for the energy of 30MeV

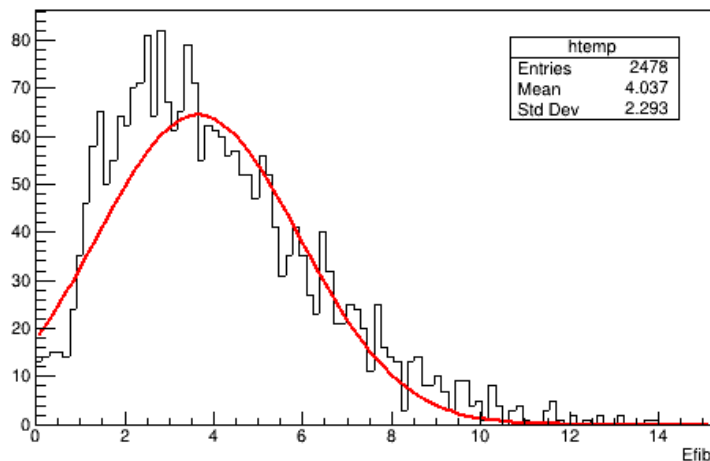


Fig. 5.3.3 Energy deposition of a shashlik type calorimeter with 4mm absorber thickness for the energy of 30MeV

The energy resolutions of the calorimeters for incident particle energy of 30 MeV, and absorber thickness of 3mm, 2mm, and 4mm respectively can be estimated as:

$$\frac{\sigma(E)}{E} = 7.84\% (3mm)$$

$$\frac{\sigma(E)}{E} = 8.38\% (2mm)$$

$$\frac{\sigma(E)}{E} = 7.59\% (4mm)$$

6. Conclusion

In this report, five different types of calorimeters were proposed: homogeneous calorimeter with LYSO scintillator crystal, spaghetti type heterogeneous calorimeter with Cu+W compound absorber and LYSO scintillator rods, as well as three different heterogeneous shashlik types of the same materials, with different absorber thicknesses. The dimensions of the calorimeters were chosen based on the calculated value of the particle shower maximum and Moliere radius. The dimensions of fibers and layers in heterogeneous calorimeters were chosen so that they make up about 24% for spaghetti and 20%, 25%, and 30% of the total calorimeter volume for the shashlik calorimeters.

The energy resolution was calculated for incident particle energy of 20, 30, 40, 50, and 100 MeV for all of the heterogeneous calorimeters.

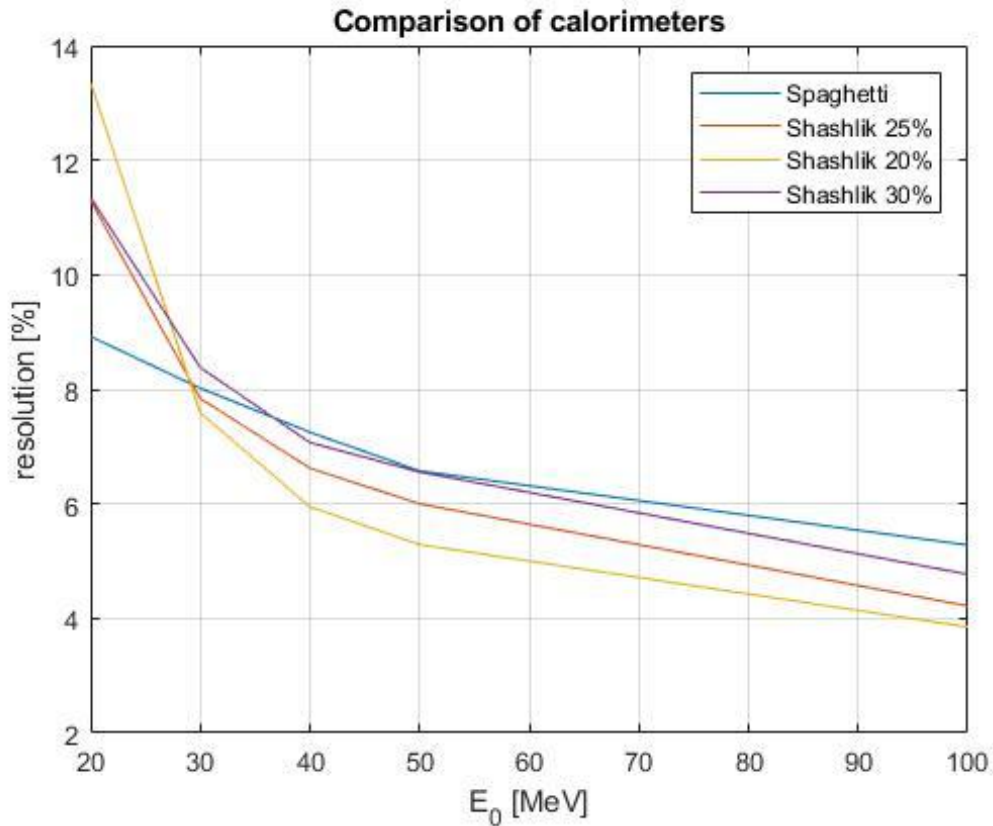


Fig. 6.1. Comparison of different calorimeters

For low energies, the spaghetti type calorimeter has the best resolution, which gets smaller towards the higher energies as expected. Unlike spaghetti, shashlik type calorimeters,

especially shashlik with 20% scintillator crystal, have a very rapid fall in energy resolution from the smallest to the largest energy considered for small photons.

The 20% shashlik calorimeter is the least expensive one and has the best performance at the energy around 100 MeV, therefore even though it would not be the best choice for soft photons it can still be valuable for a specific range detection.

The main goal of this report is to simulate and consider different models of electromagnetic calorimeters for soft photon detection. It is shown that shashlik type calorimeter using LYSO scintillator crystals and Cu+W compound, where the ratio of their thicknesses is 1:3 (25% of scintillator crystal), gives the best compromise between performances on low and high energies as well as the amount of crystal used, and therefore the price.

7. References

- [1] C. Grupen and B. Shwartz. Particle detectors (Cambridge University Press, New York, 2011)
- [2] P.V. Chliapnikov et al., Phys. Lett. B 141, 276 (1984).
- [3] D. Cockerill. Introduction to Calorimeters. Southampton Lecture, 4 May 2016.
- [4] S. Masciocchi. Electromagnetic calorimeters (GSI and University of Heidelberg). Heidelberg, 28 June 2017.

8. Acknowledgments

I would like to express my sincere gratitude for my supervisor, prof Elena Kokoulina, for introducing me to calorimetry and GEANT4, as well as guiding me through the simulation of different calorimeters and discussing the results with me.